Coil Expansion in Polyelectrolyte Solutions

Dirk Stigter

Western Regional Research Center, ARS, USDA, Berkeley, California 94710.
Received September 11, 1981

ABSTRACT: This paper discusses nonideal coil statistics. Intrachain interactions, treated in terms of the second virial coefficient of long rods, are expressed as an effective chain diameter d_B. Spherical and ellipsoidal coil models and short-chain statistics are tested with light scattering data for several series of substituted, uncharged polystyrenes. Small, unexpected trends of d_B with polymer weight are considered to be within the experimental errors of light scattering. For polymers in a good solvent, poly(*p*-methylstyrene) in toluene, results for d_B are about equal to the structural chain diameter. In poor solvents d_B is found to be much smaller. Current theories of the charge effect on the effective diameter d_B and on the persistence length P of highly charged flexible rods are reviewed and incorporated in the coil statistics of polyelectrolytes in aqueous salt solutions. The comparison of the theory with coil sizes from light scattering of poly(styrenesulfonates) shows good agreement between 0.05 and 0.5 M NaCl. At lower ionic strength, where coils are highly expanded, there is a discrepancy, suggesting that experiments at lower polyelectrolyte concentrations are needed.

1. Introduction

The subject of this paper is the electrostatic expansion of polyelectrolyte coils in aqueous salt solutions. Formally, this problem has much in common with the excluded volume effect in the statistics of uncharged polymers. In both cases the theory consists of three elements, first the persistence length of the flexible chain, secondly the repulsion between nonsequential segments of the chain, and finally, the distribution of the chain elements over the coil volume.

Odijk and Houwaart[1] and Fixman and Skolnick[2] have treated the excluded volume effect of polyelectrolytes with a line charge model, using the Debye–Hückel approximation in the electrostatic repulsions. In recent work on the electrostatic stiffening of highly charged chains[3] and on the interaction between highly charged rods,[4] the line charge model has been replaced by that of a charged cylinder, and the Debye–Hückel approximation has been eliminated. In the following these improvements are incorporated in the theory of the coil expansion of polyelectrolytes.

The statistical basis is the Hermans–Overbeek procedure.[5] Since the segment distribution cannot be derived rigorously, we investigate several approximate models. The segment interaction is introduced in terms of the second virial coefficient. Here the kinked rod model has an important advantage over the alternative, a pearl necklace model. The virial expansion for rods converges much faster than that for spheres.[6] Consequently, where in a pearl necklace coil model the third virial coefficient might be important,[7] its contribution is probably insignificant in a kinked rod model with repulsive interactions between long, cylindrical segments. Another fortunate feature is that the (total) interaction free energy in the Hermans–Overbeek expression is independent of the length of the interacting segments. In fact, the only interaction parameter is d_B, the effective diameter of the chain for pairwise segment interactions.

Apart from the coil model, the theory now has two parameters, the persistence length P and the effective chain diameter d_B. Both parameters are independent of the chain length L. In comparing with experiments, this invariance of d_B is used as a test of the theory.

The theory is first applied to uncharged polymers, several series of substituted polystyrenes. For these polymers light scattering under Θ conditions yields P. This result is used in subsequent calculations of d_B from the expanded coil size under non-Θ conditions.

For polyelectrolytes the tests of the theory are more elaborate. Here the effective diameter d_B contains an electrostatic contribution which is calculated for the particular system. The result is then used in the evaluation of the persistence length P from the experimental coil size. This "experimental" value of P should be independent of the molecular weight of the polyelectrolyte. In addition, the experimental values of P are compared with the theoretical results of P for the particular chain in the solutions under study.

2. Statistics and Interactions in Single Polymer Coils

We first review the coil statistics introduced by Hermans and Overbeek[5] and the virial method for the segment interactions. These elements form the starting point of earlier excluded volume treatments[8,9] and deserve some amplification.

The statistics is expressed in terms of the contour length L of the wormlike chain, its persistence length P, and the free energy of interaction F between all unconnected chain segments. For random flight coils, $F = 0$, P corresponds to half the length of the Kuhn statistical chain element.[9] The size of the coil is related to its radius of gyration s and to the end-to-end distance h of the coiled chain.

Following Hermans and Overbeek,[5] the mean-square values of h and s are

$$\langle h^2 \rangle = \frac{\int_0^\infty h^4 \exp\left(-\frac{3h^2}{4LP} - \frac{F}{kT}\right) dh}{\int_0^\infty h^2 \exp\left(-\frac{3h^2}{4LP} - \frac{F}{kT}\right) dh} \quad (1)$$

$$s^2 = (\langle h^2 \rangle + 2LP)/12 \quad (2)$$

Equation 1 implies that the distribution of h around the average is Gaussian, as for freely jointed chains in the limit $L/P \to \infty$. To test this approximation the Gaussian factor in eq 1, $\exp(-3h^2/4LP)$, may be replaced by the corresponding factor from the more general theory[10]

$$(\beta L/3h)(\beta^{-1} \sinh \beta)^{L/2P} \exp(-\beta h/2P) \quad (3)$$

where

$$\beta = 3(h/L) + 1.8(h/L)^3 + (297/175)(h/L)^5 + \ldots \quad (4)$$

We shall concentrate on eq 1 and use eq 3 only for some error tests.

In the free energy F we consider only pairwise interactions between polymer segments and derive F from nonideal gas theory.[11] The product PV contributes to the total free energy of the gas. The contribution of the intermo-

lecular pair interactions is given by the second term of the virial expansion

$$PV = kTV(\rho + B_2\rho^2 + ...) \quad (5)$$

The virial method carries over in dilute solution theory following McMillan and Mayer,[11,12] with the osmotic pressure replacing P. By analogy we take for the segment pair interactions in the polymer coil

$$F/kT = B_2\rho^2V \quad (6)$$

where ρ is the concentration of the chain segments in the coil volume V and B_2 is now the second virial coefficient describing the interaction between two polymer segments in the particular solvent. Since in a real polymer coil ρ is not uniform, the obvious generalization of eq 6 is

$$F/kT = B_2\int_{coil}\rho^2\,dV \quad (7)$$

The substitution in eq 1 for F from eq 7 produces the starting expression of the excluded volume treatment of uncharged polymers by Kurata, Stockmayer, and Roig.[8]

The expression of B_2 for long straight rods of length l and diameter d_B is[13]

$$B_2 = (\pi/4)l^2d_B \quad (8)$$

The application of eq 8 in eq 7 requires some comment. For chain segments d_B is an effective diameter which depends on their interaction. For curved segments eq 8 is valid as long as the simultaneous occurrence of more than one contact between a pair is infrequent.[6] Although end effects are signicant for short rods, they should be unimportant for segments of a long chain.

We now return to eq 1. We take for $\langle h^2\rangle$ the value for which the expression $h^3\exp(-3h^2/4LP - F/kT)$ is maximal. Numerical integrations have confirmed for a variety of cases that this well-known approximation, due to Hermans and Overbeek,[5] gives h values which are accurate to better than 2%. The approximation has the advantage that with eq 7 and 8 it yields a simple expression for d_B

$$d_B = \frac{12}{\pi}\left(\frac{1}{h} - \frac{h}{2LP}\right)\Big/\frac{d}{dh}\int l^2\rho^2\,dV \quad \text{at } h^2 = \langle h^2\rangle \quad (9)$$

The segment concentration ρ is always proportional to the total number of segments in the chain, L/l. As a consequence, the segment length l cancels in eq 9 for d_B. The exact segment distribution in polymer coils is not known. Therefore we discuss several approximate coil models, all having the same radius of gyration s.

In the uniform sphere model the L/l segments are distributed uniformly in a sphere with radius $s(5/3)^{1/2}$. This gives with eq 2 and 9

$$d_B = \frac{137.7s^5}{L^3P}\,\frac{3s^2 - LP}{6s^2 - LP} \quad (10)$$

In Θ solutions, where $P = 3s^2/L$, eq 10 gives $d_B = 0$, that is, no interaction, as expected.

A different segment distribution is that of the random flight coil. For large L/P the average segment conentration at distance r from the center is according to Debye and Bueche[14]

$$\rho(r) = \frac{L}{s^3l}\left(\frac{3}{4\pi}\right)^{3/2}\int_0^1 \frac{\exp\left(-\dfrac{3r^2}{4s^2\{u^3 + (1-u)^3\}}\right)}{\{u^3 + (1-u)^3\}^{3/2}}\,du \quad (11)$$

Numerical integration in eq 9 yields for this nonuniform spherical model

$$d_B = \frac{175.3s^5}{L^3P}\,\frac{3s^2 - LP}{6s^2 - LP} \quad (12)$$

Note that this result differs from eq 10 only by a numerical factor $1.273 = 4/\pi$, suggesting that in eq 9 an analytic integration can be performed with eq 11 for ρ.

The third model is that of an ellipsoidal coil. On the average a polymer coil is elongated in the direction of the end-to-end vector of the chain. Kurata et al.[8] have investigated the model of a uniformly filled ellipsoid of revolution with the same principal radii of gyration as the average coil. From their results one obtains the semiaxes a, b, and c of the ellipsoid

$$a^2 = b^2 = (5/18)LP \quad (13a)$$

$$c^2 = (5/36)(2LP + 3\langle h^2\rangle) \quad (13b)$$

For this uniform ellipsoidal model one obtains with eq 2 and 9

$$d_B = \frac{4.417(9s^2 - LP)^{3/2}}{L^2}\,\frac{3s^2 - LP}{6s^2 - LP} \quad (14)$$

The present theory has been compared with recent Monte Carlo work on the excluded volume problem of intermediate-size DNA by Post and Zimm.[15] In their preliminary computations finite values of the chain diameter d_B increased the root-mean-square radius of gyration s of the DNA coil up to 9 ± 2%. These Monte Carlo results agreed well with the present theory, eq 10 for the uniform sphere performing somewhat better than eq 12 and 14 for the other models.

Before discussing polyelectrolyte coils in more detail, we first test the statistical theory with data on several substituted polystyrenes for which the excluded volume effect may increase the radius of gyration up to 60%.

3. Coil Statistics of Polystyrenes

Light scattering of dilute polymer solutions gives information on the polymer weight M and on the mean-square radius of gyration s^2 of the polymer coil. We assume that for polystyrenes the persistence length P is independent of solvent and temperature and may be obtained from light scattering under Θ conditions as

$$P = 3(s^2)_\Theta/L \quad (15)$$

In the fully streched polymer each C–C bond in the chain contributes $a_c = 1.26$ Å to the contour length L. For the somewhat crinkled polystyrene chains with hindered rotations, L is calculated with the slightly smaller, more realistic value $a_c = 1.1$ Å. In fact, the results and arguments below are rather insensitive to the exact value of a_c. This completes the information required to derive the effective chain diameter d_B for the various coil models.

Light scattering data on series of polystyrenes and of three substituted polystyrenes were taken from the literature.[16-18] Table I shows that the persistence length P of the polystyrenes is about 12 Å and does not depend significantly on the nature of the para substituent.

Figure 1 gives the results for d_B obtained with the uniform spherical distribution of eq 10, and for the poly(p-methylstyrenes) also with the ellipsoidal distribution of eq 14. The three substituted polystyrenes exhibit a slight trend toward smaller d_B for longer chains. To examine the significance of this trend, d_B was averaged in each series, and with this average value, given in Table I, s was calculated and compared with light scattering results.

Table I
Persistence Length P and Effective Chain Diameter d_B from Light Scattering for Various Polystyrene Solutions

ref	polymer	P, Å	d_B,[c] Å		
		eq 15	eq 10	eq 12	eq 14
16	polystyrene[a]	11.6	0.72	0.92	0.94
18	poly(*p*-bromostyrene)[b]	12.7	0.83	1.05	1.07
18	poly(*p*-chlorostyrene)[b]	11.9	4.27	5.44	4.78
17	poly(*p*-methylstyrene)[b]	12.4	11.6	14.8	10.2

[a] In butanone at 22 °C. [b] In toluene at 30 °C. [c] Average values.

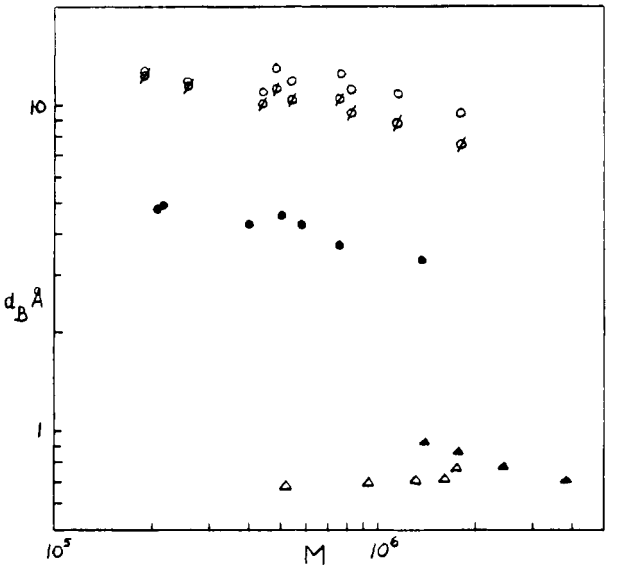

Figure 1. Effective chain diameter for segment pair interaction, d_B, vs. polymer weight M as calculated from light scattering: (△) polystyrene in butanone at 22 °C;[16] (▲) poly(*p*-bromostyrene) in toluene at 30 °C;[18] (●) poly(*p*-chlorostyrene) in toluene at 30 °C;[18] (○,∅) poly(*p*-methylstyrene) in toluene at 30 °C.[17] (△, ▲,●,○) Spherical coil model, eq 10; (∅) ellipsoidal coil model, eq 14.

Figure 2 shows s vs. $M^{1/2}$ for the poly(*p*-methylstyrenes). The calculated curves coincide with the experimental points within the errors of the light scattering data. Similar agreement was found for the other polymer series in Figure 1. The conclusion is that d_B is constant in each polymer series, at least at the present level of experimental accuracy.

In Figure 2 the lines for the uniform and the nonuniform sphere are identical, because the functional relations between d_B and s in eq 10 and 12 are the same. The influence of coil shape in Figure 2 is minor. In additional computations based on the short-chain statistics of eq 3 and 4, s was found to decrease by less than 0.5%. In summary, the differences between the various coil models discussed above are smaller than the present experimental errors in light scattering.

Table I shows that d_B is of the order of the chain diameter or smaller, as expected for uncharged polymers. There is at present no theory for predicting these d_B values. This is different in polyelectrolyte solutions. The next section reviews recent theoretical results on the effective diameter and the persistence length of polyelectrolyte chains.

4. Electrostatic Interactions in Polyelectrolyte Coils

It is well-known that many properties of polyelectrolyte

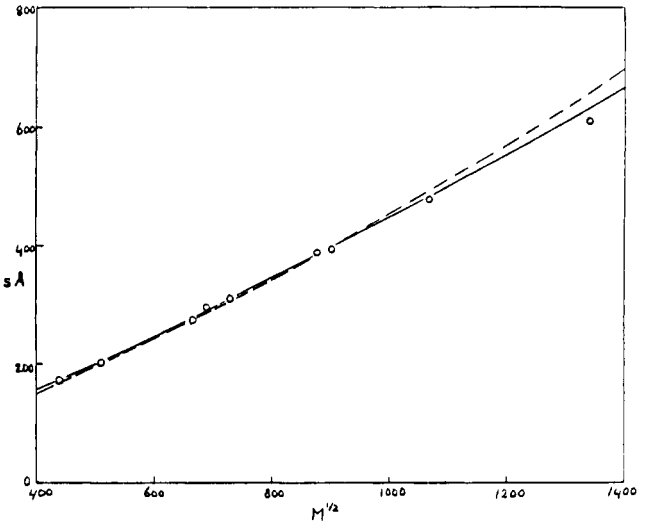

Figure 2. Radius of gyration s as a function of polymer weight M for poly(*p*-methylstyrenes). Open circles from light scattering in toluene at 30 °C.[17] Solid curve from eq 10 for spherical coil model, with P = 12.4 Å and d_B = 11.6 Å. Dashed curve from eq 14 for ellipsoidal model, with P = 12.4 Å and d_B = 10.2 Å.

solutions depend markedly on the concentration of added salt, demonstrating the importance of electrostatic interactions. The range of these interactions is measured in terms of the Debye shielding length $1/\kappa$, which changes from about 10 Å in 0.1 M NaCl solution to about 100 Å in 0.001 M NaCl solution at room temperature.

From a theoretical point of view it is helpful to classify the interactions according to range and intensity as follows. (a) Short-range electrostatic interactions, $<1/\kappa$, operate on the adsorption of small ions to the chain, including the titration of constituent acidic and basic groups. The effects are up to several kT per adsorbed ion. (b) Electrostatic repulsion between vicinal, fixed charges along the chain increases the stiffness of the chain. These interactions are medium range, $\approx 1/\kappa$, and they increase the persistence length P_0 of the uncharged chain to $P = P_0 + P_{el}$. For highly charged chains P_{el} may be several times $1/\kappa$. The electrostatic straightening of a kinked chain decreases its conformational entropy by about k for every kink that is removed, or of order $0.1kT$ for the free energy per fixed charge. (c) Long-range electrostatic repulsions, $>1/\kappa$, between different, nonsequential chain segments expand the volume of the coil. As reported later, these interactions may contribute per fixed charge of the order of $0.001kT$ to the free energy F in eq 1 and 7.

The three effects just described all deal with equilibrium properties. Hence, their theoretical treatment involves minimizing the free energy of the system. Fortunately, the various effects are quite different so they may be uncoupled and treated separately. More precisely, the coordinates describing the three effects are fairly independent of one another, and it is a reasonable approximation to minimize the free energy with respect to the three phenomena in sequence instead of simultaneously. For this reason it is not inconsistent to use different models and different approximations for the various parts of the electrostatic interaction curve. We proceed as follows.

The strong, short-range attractions are dealt with on an empirical basis; that is, the polymer charge, Ze per unit length, is derived from experimental data on titration or electrokinetics.

The electrostatic contribution P_{el} to the persistence length P is taken from the recent work of Le Bret for a highly charged, flexible rod, modeled as a toroid and

Table II
Correction Factor β of Debye-Hückel Charge Potential Relation as a Function of Radius x_0 and Surface Charge Density ξ/x_0 of Colloidal Cylinder in 1:1 Salt Solution[a,b]

	ξ/x_0								
x_0	3	6	9	12	15	18	21	24	27
16	1.613	2.344	3.024	3.667	4.282	4.876	5.454	6.018	6.570
8	1.580	2.286	2.945	3.568	4.166	4.743	5.304	5.851	6.388
4	1.522	2.183	2.805	3.394	3.959	4.506	5.037	5.556	6.064
2	1.430	2.017	2.577	3.110	3.623	4.120	4.602	5.074	5.536
1	1.306	1.783	2.253	2.705	3.141	3.565	3.978	4.381	4.777
1/2	1.175	1.509	1.863	2.213	2.555	2.888	3.214	3.533	3.846
1/4	1.074	1.257	1.483	1.722	1.961	2.198	2.432	2.663	2.890
1/8	1.024	1.093	1.199	1.329	1.470	1.616	1.765	1.915	2.064
	ξ/x_0								
x_0	12	15	18	21	24	27	30	33	36
1/16	1.104	1.161	1.229	1.303	1.383	1.466	1.551	1.637	1.724
1/32	1.025	1.039	1.058	1.080	1.107	1.137	1.170	1.207	1.246
1/64	1.005	1.009	1.013	1.017	1.023	1.030	1.037	1.046	1.055

[a] Radius x_0 in units of $1/\kappa$. [b] Linear charge density $\xi = Ze^2/DkT$ for cylinder with charge Ze per Å.

Table III
Correction Factor γ of Debye-Hückel Potential Distance Relation as a Function of Radius x_0 and Surface Charge Density ξ/x_0 of Colloidal Cylinder in 1:1 Salt Solutions[a,b]

	ξ/x_0								
x_0	3	6	9	12	15	18	21	24	27
16	1.248	1.453	1.595	1.705	1.794	1.869	1.933	1.990	2.041
8	1.237	1.436	1.577	1.685	1.772	1.846	1.909	1.966	2.016
4	1.217	1.409	1.545	1.650	1.735	1.807	1.869	1.924	1.973
2	1.186	1.366	1.496	1.596	1.678	1.747	1.806	1.859	1.906
1	1.143	1.305	1.426	1.520	1.597	1.662	1.719	1.769	1.813
1/2	1.094	1.229	1.338	1.425	1.496	1.557	1.610	1.656	1.698
1/4	1.048	1.144	1.236	1.314	1.380	1.436	1.485	1.528	1.566
1/8	1.019	1.069	1.133	1.196	1.253	1.304	1.349	1.389	1.425
	ξ/x_0								
x_0	12	15	18	21	24	27	30	33	36
1/16	1.090	1.129	1.169	1.207	1.243	1.276	1.307	1.335	1.361
1/32	1.030	1.046	1.065	1.086	1.109	1.132	1.155	1.179	1.201
1/64	1.009	1.014	1.019	1.026	1.034	1.043	1.053	1.063	1.075

[a] Radius x_0 in units of $1/\kappa$. [b] Linear charge density $\xi = Ze^2/DkT$ for cylinder with charge Ze per Å.

surrounded by a Gouy ionic atmosphere.[3] His results are written as

$$P = P_0 + P_{el} = P_0 + \frac{Z^2e^2}{4DkT\kappa^2}Y \qquad (16)$$

where Y is a numerical factor. For $Y = 1$ eq 16 applies to a line charge with a linear charge density Ze which is low enough for linearization of the Poisson–Boltzmann equation, the case treated by Odijk[19] and by Skolnick and Fixman.[20] In general, Y is a function of Z, of the radius r_0 of the rod, and of the Debye length $1/\kappa$. Le Bret has computed P_{el} for a range of conditions.[3]

We proceed with the free energy of interaction F between the charged segments, that is, the excluded volume effects due to weak, long-range electrostatic repulsions as expressed in the effective chain diameter d_B. We combine two earlier treatments[2,4] of the electrostatic repulsion between two long, randomly oriented rods. The general result for the effective rod diameter d_B is in terms of a contact potential w

$$d_B = d + (1.2634w - 0.4170w^2 + 0.1007w^3 - 0.0107w^4)/\kappa \quad \text{for } w < 3.5 \qquad (17)$$

$$d_B = d + (\ln w + \gamma' - 1/2 + \ln 2)/\kappa \quad \text{for } w > 3 \qquad (18)$$

where γ' is Euler's constant and $\gamma' - 1/2 + \ln 2 = 0.7704$. For $w = 0$ eq 17 gives for d_B the hard-rod diameter $d = 2r_0$. For charged rods

$$w = \frac{Z^2e^2}{DkT\kappa}\frac{2\pi e^{-2x_0}}{\{\beta\gamma x_0 K_1(x_0)\}^2} \qquad (19)$$

In eq 19 K_1 is a modified Bessel function of argument $x_0 = \kappa r_0$; β and γ are correction factors of the Debye–Hückel theory, given in Tables II and III and discussed further in the Appendix.

Relations of eq 17–19 with the earlier work are simple. Equation 18 holds for highly charged rods when actual contacts between the rods are unlikely. The previous treatment of this case[4] was in terms of the variable w $\exp(2x_0)$, denoted F, and the dimensionless surface potential y_0 of the rods. The replacement of y_0 by Ze introduces the factor β in eq 19.[21]

Fixman and Skolnick specifically exclude overlap of the rods also for weak repulsion. Their results are given in terms of a function $R(w)$ which is tabulated.[2] The polynomial in eq 17 is a convenient representation of $4R(w)/\pi$, accurate to better than 0.5%. For nonoverlapping rods ref 2 introduces the Debye–Hückel repulsion between line charges, that is, eq 20 with $\beta = \gamma = 1$, and using for all x_0 the value $x_0K_1(x_0) = 1$, one obtains the limit for $x_0 = 0$.

We compare the treatment of ref 2 with results for rods with a Gouy double layer, the model of eq 17–19. The comparison is for rods with diameter $d = 9$ Å and linear

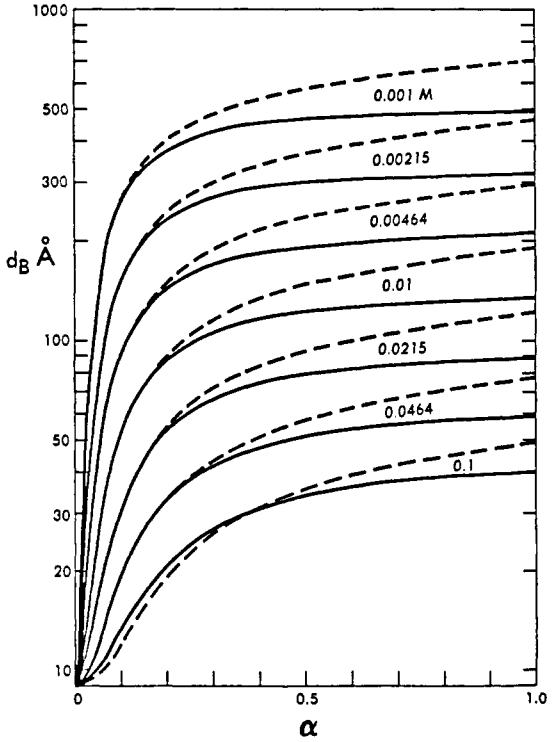

Figure 3. Effective diameter d_B vs. degree of ionization α of charged rod with diameter $d = 9$ Å and linear charge density $Ze = \alpha e/2.4$ Å. Solid lines for present theory with Gouy model, eq 17–19. Dashed lines for treatment by Fixman and Skolnick based on repulsion between line charges and Debye–Hückel approximation.[2]

charge density $Ze = \alpha e$ per 2.4 Å, corresponding roughly to poly(methacrylic acid) with degree of neutralization α, in NaCl solutions. The results in Figure 3 show that for low α and not too high ionic strength the theories merge, while for high α the differences are significant.

In the earlier paper[4] values of d_B for double-stranded DNA in NaCl solutions were predicted. These theoretical results are in excellent agreement with the effective diameters of fragments of sheared DNA determined by Brian, Frisch, and Lerman[22] in sedimentation equilibria.

5. Comparison of Theory and Experiment

In the preceding sections we have discussed the three elements that determine the size of polyelectrolyte coils, namely, coil statistics, persistence length of the chain, and repulsion between nonsequential chain segments. The statistics and the repulsion theory have survived the limited tests with available experiments. We now proceed with an overall test of the theory, using data on sodium poly(styrenesulfonates) by Takahashi et al.[23] Table IV shows radii of gyration s as a function of NaCl concentration derived from light scattering experiments on three samples of different molecular weight.

As in Figure 1, the theoretical contour length L of the polymers is based on 1.1 Å per C–C bond in the chain. For the hard-core chain diameter we take the structural value $d = 14$ Å. We assume complete ionization, taking $Ze = e$ per 2.2 Å. With this chain model the theory may be compared with the experiments in several ways.

As a first step we test the mutual consistency of the sets of s values for the three polymer samples in Table IV. To this end we evaluate d_B from the chain model (see Figure 5), substitute the results in eq 12 along with the corresponding s values from Table IV, and solve for P. The results, shown in Figure 4, should not depend significantly on the polymer weight. In fact, the vertical spread between

Table IV
Radius of Gyration, $s = \langle s^2 \rangle_z^{1/2}$, of Sodium Poly(styrene-*p*-sulfonate) in NaCl Solutions from Light Scattering by Takahashi et al.[23]

	s, Å		
c_{NaCl}, M	$(2.28 \pm 0.05) \times 10^6$[a]	$(1.55 \pm 0.05) \times 10^6$[a]	$(1.00 \pm 0.05) \times 10^6$[a]
0.5	710	590	471
0.1	842	716	591
0.05	947	799	637
0.02	1085	834	659
0.01		863	692
0.005	1104	945	706
			190[b]

[a] Molecular weight. [b] 3.1 M KCl, Θ point.

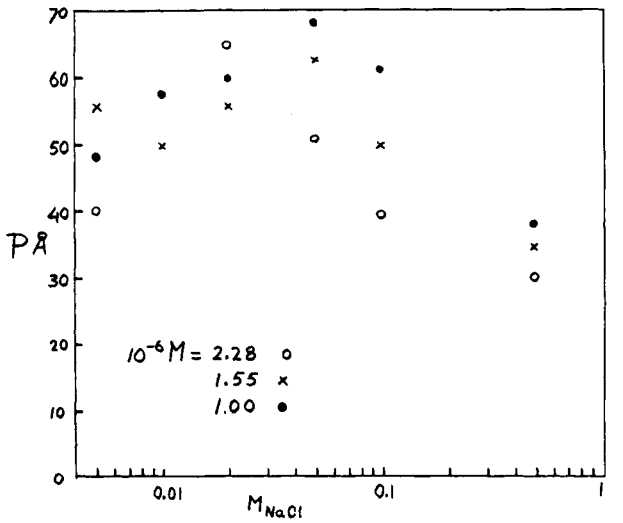

Figure 4. Persistence length P of sodium poly(styrenesulfonates) as function of ionic strength, evaluated from eq 12 for the Gaussian coil, with radii of gyration s of Table IV and effective chain diameters d_B of Figure 5.

the points in Figure 4 corresponds to about a 5% variation in s. This probably equals the experimental uncertainty, meaning that the differences are not significant. The other coil models of eq 10 and 14 gave very similar results.

For the second step the results of P for the three polymer samples are averaged. These averages, denoted P_{exptl}, are shown vs. the NaCl concentration as dashed curves in Figure 5. These curves are compared with the solid curve of P_{theor}, which was computed for the chain model from eq 16, with estimates of Y according to Le Bret[3] and the value of P under Θ conditions, $P_0 = 10$ Å, from eq 15 and Table IV. For high ionic strength, $c_{NaCl} > 0.05$ M, there are no great differences between P_{exptl} and P_{theor}, suggesting that the present theory of coil swelling works reasonably well in this range. However, P_{exptl} decreases in more dilute salt solutions, exhibiting an increasing discrepancy with P_{theor}. The anomalous maximum of P_{exptl} persists in all three models upon variation of the chain parameters for the computation of d_B and L (charge density, hard-core diameter, or contour length per monomer), while P_{theor} never shows a maximum. Three sources of error in P_{exptl} suggest themselves.

First, eq 17–19 for the computation of d_B assume interaction between two long straight rods. Now, the chain is not straight on the scale of d_B since in dilute salt solutions $P_{theor} < d_B$; see Figure 5. Therefore, the results for d_B are probably too high. Using smaller values of d_B in eq 10, 12, or 14 will give higher results for P_{exptl}. This was tested by using eq 10–14 with P_{theor} and the s values of

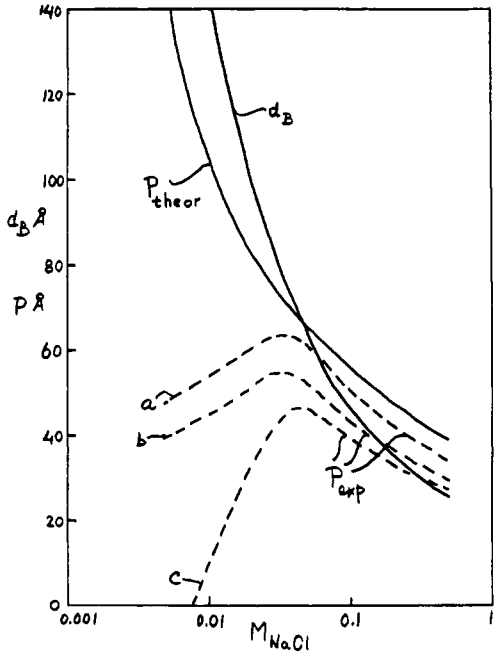

Figure 5. Chain parameters of sodium poly(styrenesulfonates) as a funcion of ionic strength. Effective chain diameter d_B from eq 17–19, and persistence length P_{theor} from eq 16 for chain model defined in text. Curve a for the Gaussian coil, eq 12, is taken from the data of Figure 4, after averaging for the three molecular weight samples. Curves b and c are similar averages for the uniform sphere, eq 10, and for the ellipsoidal coil, eq 14, again based on the information on s in Table IV and on d_B in this figure.

Table IV to obtain d_B as functions of the ionic strength. Such functions showed in all cases an anomalous maximum of d_B. The conclusion is that reasonable adjustment of d_B as input in eq 10, 12, or 14 cannot overcome the large discrepancies between P_{exptl} and P_{theor} in Figure 5.

The second source of possible error is the coil statistics of eq 1 for highly swollen coils. This was checked with the stiff-chain statistics in eq 3 and 4. It was found that the factor $\exp(-3h^2/4LP)$ in eq 1 is at most 5.8% too high, while $h/L < 0.19$ in all cases of Table IV. So there is no reason to suspect that the coil statistics is the main source of the discrepancy.

A third possibility is the experimental determination of s. The data in Table IV were derived from the dissymmetry of light scattering at five different polymer concentrations from 0.3 to 0.05 g/mL. For given polymer weight and concentration it is simple to calculate the coil size for which the solution is completely filled with polymer coils, without overlap between neighboring coils. For the lowest experimental polymer concentration of 0.05 g/100 mL, this coil size corresponds to s = 716, 829, and 943 Å for the experimental polymer weights $M = 1 \times 10^6$, 1.55×10^6, and 2.28×10^6, respectively. It is obvious from Table IV that most of the light scattering experiments were carried out at too high polymer concentrations, where the coils were not fully expanded or else intertwined, in particular for the lower ionic strength solutions. It is unlikely that the light scattering dissymmetry in such solutions extrapolated to the correct value of s at infinite dilution of polymer. Too low values of s in Table IV are probably the main cause of the unexpected maxima of P_{exptl}.

Finally, the free energy of interaction between the chain segments was computed from eq 7 for the solutions under study. Typically, for ellipsoidal coils, with $h^2 = \langle h^2 \rangle$, F was found to be around $10kT$ per coil, that is, of order $10^{-3}kT$ per fixed charge, and somewhat dependent on the ionic strength.

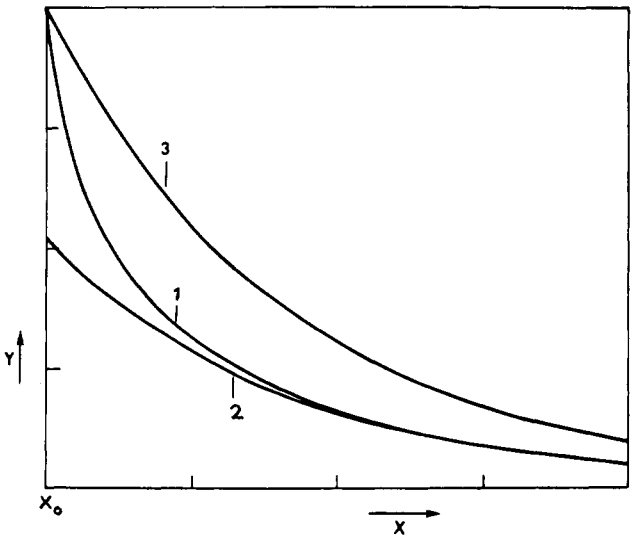

Figure 6. Potential–distance curves around a charged cylinder in salt solution. Curve 1 from full Poisson–Boltzmann equation. Curves 2 and 3 from linearized Poisson–Boltzmann equation.

6. Concluding Remarks

It is useful to enumerate the lacunae and shortcomings in the currently available theory and experiments.

There is a lack of suitable light scattering experiments carried out at sufficiently low polymer concentrations. Coil size determinations from viscosity data[9] are unreliable for charged polymers because there is at present no theory to correct the viscosity data for charge effects.

The theory in this paper overestimates the intersegment repulsion, because it is based on the interaction between long, straight, charged rodds. For flexible polyelectrolytes, where $d_B > P$ as in Figure 5, an improved theory would treat the repulsion between curved rods. The novel part of such a theory would extend the treatment of Fixman and Skolnick[2] to curved line charges. The application to curved rods and the elimination of the Debye–Hückel approximation would merely replace the line charge density Ze by $Ze/\beta\gamma x_0 K_1(x_0)$, as in eq 19. As explained earlier,[4] this is because the region in which the repulsion originates is located far from the line charge where the Debye–Hückel linearization of the Poisson–Boltzmann eq is valid.

The computations for poly(styrenesulfonate) in this paper are based on the structural chain diameter and on the titration charge. It would be more satisfactory to use the hydrodynamic chain diameter and the electrophoretic charge density. However, the necessary transport experiments are not available for poly(styrenesulfonate).

It would be interesting to use double-stranded DNA as a test system. The advantage is that there is fairly good information available on the hydrodynamic diameter and on the kinetic charge of DNA.[24] Moreover, the double helix is so stiff that the current theory on intrachain interactions may be used with some confidence and already has experimental support.[22] The persistence length may present more problems because theoretical results are quite sensitive to details of the assumed model[3] and experimental values are difficult to obtain in a direct way.

The most important part missing from the theory is perhaps the configurational statistics of relatively short chains. The segment pair density ρ^2 in eq 7 should vanish well before the limit $h/L = 1$ is reached. It might be necessary to abandon the approach for spherical coils in eq 1 altogether and use instead, for instance, an extension of the work of Wall and Seitz[25] on the asymptotic behavior of chains with limited orders of non-self-intersection.

Acknowledgment. This research was carried out partly during a 3-month visit with the Colloid Research Group of Professor J. Lyklema at the Agricultural University of Wageningen, supported by the Netherlands Organization for Pure Scientific Research (ZWO). During this visit the author has benefited greatly from discussions with Professor J. Th. G. Overbeek and Dr. T. Odijk. Thanks are due also to Professor J. A. Schellman and Professor B. H. Zimm for comments on an early version of the paper and to Carol Post, Professor Lerman and Dr. Le Bret for making results available prior to publication.

Appendix

The factors β and γ are defined with the help of Figure 6, which shows three potential–distance curves around a charged cylinder in a salt solution; $y = e\psi/kT$ is the dimensionless potential and $x = \kappa r$ is the distance from the axis in units of $1/\kappa$. Curve 1 is a computer-generated solution of the full Poisson–Boltzmann equation. Curves 2 and 3 are solutions of the linearized Poisson–Boltzmann equation; both curves are proportional to the Bessel function $K_0(x)$. At the surface of the cylinder, at $x = x_0$, curves 1 and 3 both start at $y_1(x_0) = y_3(x_0)$, while at large distance, $y_1(x) = y_2(x)$, for $x \to \infty$.

The factor γ is defined as

$$\gamma = \frac{y_3(x)}{y_2(x)} = \frac{y_1(x_0)}{y_2(x_0)} = \frac{(dy_3/dx)_{x_0}}{(dy_2/dx)_{x_0}} \tag{A1}$$

and the factor β with

$$\beta = \frac{(dy_1/dx)_{x_0}}{(dy_3/dx)_{x_0}} \tag{A2}$$

By Gauss' law the linear charge density Ze of the rod is proportional to $(dy/dx)_{x_0}$. Now, the interaction treatment leading to eq 19 assumes that curve 1 is correct but, in fact, uses curve 2, albeit only for large x. This means that, instead of the charge Ze proportional to $(dy_1/dx)_{x_0}$ we should use in eq 19 the charge proportional to

$$(dy_2/dx)_{x_0} = \left(\frac{dy_1}{dx}\right)_{x_0} \frac{(dy_3/dx)_{x_0}}{(dy_1/dx)_{x_0}} \frac{(dy_2/dx)_{x_0}}{(dy_3/dx)_{x_0}} = \left(\frac{dy_1}{dx}\right)_{x_0} \frac{1}{\beta} \frac{1}{\gamma} \tag{A3}$$

So we have replaced Ze by $Ze/\beta\gamma$ in the derivation of eq 19.

The factors β and γ are given in Tables II and III as functions of the dimensionless radius, x_0, and surface charge, ξ/x_0, of the rod. The data have been computed from the original tables[21] of β and γ as functions of x_0 and surface potential. In many applications, when estimates of the surface charge, rather than the surface potential, are availabale, the present tables are easier to use than the earlier ones.[21]

References and Notes

(1) Odijk, T.; Houwaart, A. C. *J. Polym. Sci., Polym. Phys. Ed.* **1978**, *16*, 627.
(2) Fixman, M.; Skolnick, J. *Macromolecules* **1978**, *11*, 863.
(3) Le Bret, M. *C. R. Hebd. Seances Acad. Sci., Ser. B* **1981**, *292*, 291. Additional results were kindly supplied by Dr. Le Bret.
(4) Stigter, D. *Biopolymers* **1977**, *16*, 1435.
(5) Hermans, J. J.; Overbeek, J. Th. G. *Recl. Trav. Chim. Pays-Bas* **1948**, *67*, 761.
(6) Onsager, L. *Ann. N.Y. Acad. Sci.* **1949**, *51*, 627.
(7) Post, C. B.; Zimm, B. H. *Biopolymers* **1979**, *18*, 1487.
(8) Kurata, M.; Stockmayer, W. H.; Roig, A. *J. Chem. Phys.* **1960**, *33*, 151.
(9) Yamakawa, H. "Modern Theory of Polymer Solutions"; Harper and Row: New York, 1971.
(10) Flory, P. J. "Statistical Mechanics of Chain Molecules"; Interscience: New York, 1969.
(11) Hill, T. L. "Introduction to Statistical Thermodynamics"; Addison-Wesley: Reading, Mass., 1960.
(12) McMillan, W. G.; Mayer, J. E. *J. Chem. Phys.* **1945**, *13*, 276.
(13) Zimm, B. H. *J. Chem. Phys.* **1946**, *14*, 164.
(14) Debye, P.; Bueche, F. *J. Chem. Phys.* **1952**, *20*, 1337.
(15) Post, C. B.; Zimm, B. H., personal communication.
(16) Outer, P.; Carr, C. I.; Zimm, B. H. *J. Chem. Phys.* **1950**, *18*, 830. Krigbaum, W. R.; Carpenter, D. K. *J. Phys. Chem.* **1955**, *59*, 1166.
(17) Tanaka, G.; Imai, S.; Yamakawa, H. *J. Chem. Phys.* **1970**, *52*, 2639.
(18) Noguchi, Y.; Aoki, A.; Tanaka, G.; Yamakawa, H. *J. Chem. Phys.* **1970**, *52*, 2651.
(19) Odijk, T. *J. Polym. Sci., Polym. Phys. Ed.* **1977**, *15*, 477.
(20) Skolnick, J.; Fixman, M. *Macromolecules* **1977**, *10*, 944.
(21) Stigter, D. *J. Colloid Interface Sci.* **1975**, *53*, 296.
(22) Brian, A. A.; Frisch, L. H.; Lerman. L. S. *Biopolymers*, in press.
(23) Takahashi, A.; Kato, T.; Nagasawa, M. *J. Phys. Chem.* **1967**, *71*, 2001.
(24) Stigter, D. *J. Phys. Chem.* **1979**, *83*, 1670. The conductance theory in this paper does not consider a possible contribution of the electric dipole field generated by the asymmetric charge distribution around DNA in motion. Such dipole fields require further study.
(25) Wall, F. T.; Seitz, W. A. *J. Chem. Phys.* **1979**, *70*, 1860.